INTERNATIONAL JOURNAL FOR NUMERICAL METHODS IN ENGINEERING
*Int. J. Numer. Meth. Engng* 2002; **55**:1167–1183 (DOI: 10.1002/nme.540)

# Efficient mixed Timoshenko–Mindlin shell elements

G. M. Kulikov*,† and S. V. Plotnikova

*Department of Applied Mathematics and Mechanics, Tambov State Technical University, Sovetskaya Street 106, Tambov 392000, Russia*

SUMMARY

The precise representation of rigid body motions in the displacement patterns of curved Timoshenko–Mindlin (TM) shell elements is considered. This consideration requires the development of the strain–displacement relationships of the TM shell theory with regard to their consistency with the rigid body motions. For this purpose a refined TM theory of multilayered anisotropic shells is elaborated. The effects of transverse shear deformation and bending-extension coupling are included. The fundamental unknowns consist of five displacements and eight strains of the face surfaces of the shell, and eight stress resultants. On the basis of this theory the simple and efficient mixed models are developed. The elemental arrays are derived using the Hu–Washizu mixed variational principle. Numerical results are presented to demonstrate the high accuracy and effectiveness of the developed 4-node shell elements and to compare their performance with other finite elements reported in the literature. Copyright © 2002 John Wiley & Sons, Ltd.

KEY WORDS: Timoshenko–Mindlin element; mixed model; rigid body motion; multilayered shell

## 1. INTRODUCTION

One of the main requirements of the modern shell theory that is intended for the general finite element (FE) formulation is that it must lead to strain-free modes for rigid body motions. The adequate representation of rigid body motions is a necessary condition if an element is to have good accuracy and convergence properties. Therefore, when an inconsistent theory is used to construct any finite element, erroneous straining modes under rigid body motions may be appeared. This problem has been studied for the Kirchhoff–Love shell theory by Cantin [1] and Dawe [2].

*Correspondence to: G. M. Kulikov, Department of Applied Mathematics and Mechanics, Tambov State Technical University, Sovetskaya Street 106, Tambov 392000, Russia
†E-mail: kulikov@apmath.tstu.ru

Contract/grant sponsor: Russian Fund of Basic Research; contract/grant number: 98-01-04076
Contract/grant sponsor: Research Programme of Tambov State Technical University; contract/grant number: 1Г/00-10

*Received 9 December 2000*
*Revised 1 November 2001*
*Accepted 4 February 2002*

Published online 20 August 2002

Herein, the more general study on the basis of the refined Timoshenko–Mindlin (TM) theory of multilayered shells is considered [3, 4]. The direct use of the traditional TM shell theory (the first-order shear deformation theory) [5–9] for solving a series of important shell problems such as the contact problems is not always convenient. In these problems it is more convenient to select as unknown functions the displacements of the top and bottom surfaces of the shell, since with the help of these displacements the kinematic requirement of no penetration of the contact bodies can be fulfilled. Furthermore, the proposed TM shell theory can also simplify a formulation of new FE models [10].

Using the classical linear TM shell theory in a FE formulation for plates and shells is well established and has been shown to give acceptable results [11–18]. This theory has the advantage that independent displacement and rotation trial functions may be used and these functions need only to be $C^0$ continuous. The developed FE formulation, based on the refined TM shell theory [3, 4] has the advantage because only independent trial functions of displacements of the face surfaces may be used. It should be mentioned that in some works (e.g. References [19, 20]) developing the degenerate solid shell concept [11, 21] displacement vectors of the bottom and top surfaces are also used and resolved with respect to some global Cartesian basis in order to exactly describe rigid body motions. This allows, in particular, special boundary conditions at the face surfaces of the shell to be accounted for. The same idea of selecting as unknowns the displacements of the bottom and top surfaces to construct any curved TM shell element is very attractive, since *only* in this case we can deduce linear or non-linear TM strain–displacement relationships that are free for all small or large rigid body motions, respectively. Taking into account that herein the displacement vectors of the face surfaces are represented in the local reference surface basis, the developed FE formulation has substantial computational advantages compared to the conventional isoparametric FE formulations, since it eliminates the costly numerical integration by deriving the stiffness matrices. Indeed, our element matrix requires only direct substitutions, no inversion is needed if the element is rectangular, and it is evaluated by using the full exact analytical integration.

Our FE formulation is based on a simple and efficient approximation of shells via quadrilateral 4-node elements developed by Hughes and Tezduyar [22], and by Wempner *et al.* [23]. The fundamental unknowns consist of five displacements and eight strains of the face surfaces of the shell, and eight stress resultants. The simplest admissible approximations of the two-dimensional fields are used, namely, bilinear approximations of the displacements, and assumed approximations of the strains and stress resultants. In this connection the element characteristic arrays are obtained by applying the Hu–Washizu mixed variational principle. It is worth noting that the stiffness matrix has six, and only six, zero eigenvalues as required for satisfaction of the general rigid body motion requirements.

Numerical results are presented to demonstrate the high accuracy and effectiveness of the FE models developed and to compare their performance with other FE models reported in the literature. For this purpose four tests were employed. They were pinched cylinder tests, a shell roof test, and an open cylindrical multilayered composite shell test.

## 2. STRAIN–DISPLACEMENT EQUATIONS

Let us consider a shell of uniform thickness $h$. The shell may be defined as a three-dimensional body of volume $V$ bounded by two bounding surfaces $S^-$ and $S^+$, located at distances $\delta^-$

 

and $\delta^+$ measured with respect to the reference surface $S$, and the edge boundary surface $\Omega$ that is perpendicular to the reference surface (see Figure 1). Let the reference surface $S$ be referred to an orthogonal curvilinear co-ordinate system $\alpha_1$ and $\alpha_2$ which coincides with the lines of principal curvatures of its surface; $\mathbf{e}_1$ and $\mathbf{e}_2$ denote the tangent unit vectors to the lines of principal curvatures. The $\alpha_3$ axis is oriented along the outward unit vector $\mathbf{e}_3$ normal to the reference surface.

The three-dimensional strain–displacement relationships for the general shell in a vector form can be written as

$$\varepsilon_{ii}^{\mathrm{e}} = \frac{1}{H_i}\frac{\partial \mathbf{u}}{\partial \alpha_i}\mathbf{e}_i, \quad \varepsilon_{ij}^{\mathrm{e}} = \frac{1}{H_i}\frac{\partial \mathbf{u}}{\partial \alpha_i}\mathbf{e}_j + \frac{1}{H_j}\frac{\partial \mathbf{u}}{\partial \alpha_j}\mathbf{e}_i \quad (i \neq j)$$
$$H_\alpha = A_\alpha(1 + k_\alpha \alpha_3), \quad H_3 = 1 \tag{1}$$

where $\mathbf{u} = \sum_i u_i \mathbf{e}_i$ is the displacement vector; $u_i(\alpha_1, \alpha_2, \alpha_3)$ are the components of this vector; $A_\alpha$ and $k_\alpha$ are the Lamé coefficients and principal curvatures of the reference surface; $H_\alpha$ are the Lamé coefficients of any surface parallel to the reference surface. Both here and in the following developments, unless otherwise specified, Greek indices may take the values 1, 2 while Latin indices take the values 1, 2, 3.

The refined TM shell theory is based on the linear approximation of the displacement vector in the thickness direction [3]:

$$\mathbf{u} = N^-(\alpha_3)\mathbf{v}^- + N^+(\alpha_3)\mathbf{v}^+ \tag{2a}$$

$$\mathbf{v}^\pm = \sum_\alpha v_\alpha^\pm \mathbf{e}_\alpha + v_3 \mathbf{e}_3 \tag{2b}$$

$$N^-(\alpha_3) = (\delta^+ - \alpha_3)/h, \quad N^+(\alpha_3) = (\alpha_3 - \delta^-)/h \tag{2c}$$

where $\mathbf{v}^\pm$ are the displacement vectors of the face surfaces $S^\pm$; $v_\alpha^\pm(\alpha_1, \alpha_2)$ are the tangential displacements of the face surfaces; $v_3(\alpha_1, \alpha_2)$ is the transverse displacement of the reference surface; $N^-(\alpha_3)$ and $N^+(\alpha_3)$ are the linear shape functions. The linear approximation (2) may be treated as a refined Timoshenko kinematic hypothesis (e.g. works [7, 8], where as unknown functions the displacements and rotation components of the reference surface are selected). The advantage of the proposed approach is obvious, since with the help of the displacements $v_\alpha^\pm$ the special loading conditions at the face surfaces of the shell can be formulated. Moreover, this simplifies a formulation of new FE models and provides a convenient way to express the non-linear strain–displacement relationships in terms of face surface strains [3, 10].

Substituting displacements (2a) into the strain–displacement relationships (1) and taking into account formulas for the derivatives of the unit vectors $\mathbf{e}_i$ along the co-ordinate lines $\alpha_1$ and $\alpha_2$ [24], one can obtain the following strain–displacement equations of the TM theory of the *thick* shells:

$$\varepsilon_{\gamma\gamma}^{\mathrm{a}} = \left[N^-(\alpha_3)\frac{1}{H_\gamma}\frac{\partial \mathbf{v}^-}{\partial \alpha_\gamma} + N^+(\alpha_3)\frac{1}{H_\gamma}\frac{\partial \mathbf{v}^+}{\partial \alpha_\gamma}\right]\mathbf{e}_\gamma, \quad \varepsilon_{33}^{\mathrm{a}} = 0 \tag{3a}$$

 

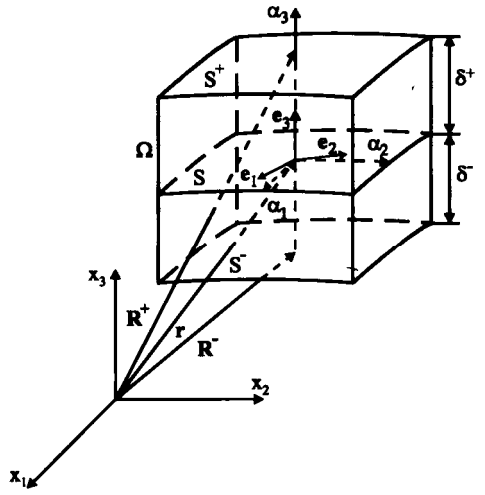


Figure 1. Shell element.

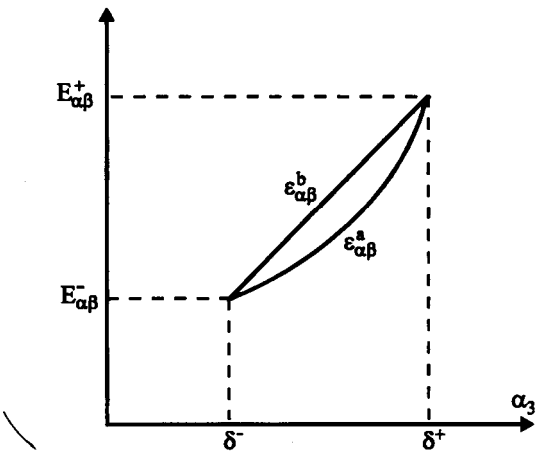


Figure 2. Distribution of tangential strains over shell thickness.

$$\varepsilon_{12}^{a}=\left[N^{-}(\alpha_3)\frac{1}{H_1}\frac{\partial \mathbf{v}^{-}}{\partial\alpha_1}+N^{+}(\alpha_3)\frac{1}{H_1}\frac{\partial \mathbf{v}^{+}}{\partial\alpha_1}\right]\mathbf{e}_2+\left[N^{-}(\alpha_3)\frac{1}{H_2}\frac{\partial \mathbf{v}^{-}}{\partial\alpha_2}+N^{+}(\alpha_3)\frac{1}{H_2}\frac{\partial \mathbf{v}^{+}}{\partial\alpha_2}\right]\mathbf{e}_1$$

$$\varepsilon_{\gamma 3}^{a}=\frac{\bar{H}_\gamma}{H_\gamma}\boldsymbol{\beta}\mathbf{e}_\gamma+\frac{1}{H_\gamma}\frac{\partial \mathbf{v}}{\partial\alpha_\gamma}\mathbf{e}_3,\quad \boldsymbol{\beta}=\frac{1}{h}(\mathbf{v}^{+}-\mathbf{v}^{-}),\quad \mathbf{v}=\frac{1}{2}(\mathbf{v}^{-}+\mathbf{v}^{+}) \tag{3b}$$

where $\bar{H}_\gamma=A_\gamma(1+k_\gamma\bar{\delta})$ are the Lamé coefficients of the middle surface; $\bar{\delta}=(\delta^{-}+\delta^{+})/2$ is the distance from the reference surface $S$ to the middle surface of the shell.

Replacing further the Lamé coefficients $H_\gamma$ by their values on the top and bottom surfaces $H_\gamma^{\pm}=A_\gamma(1+k_\gamma\delta^{\pm})$ in formulas (3a) for the tangential strains and by their values on the middle surface $\bar{H}_\gamma$ in formulas (3b) for the transverse shear strains, the strain–displacement equations of the refined TM theory of the *moderately thick* shells are obtained:

$$\varepsilon_{\gamma\gamma}^{b}=\left[N^{-}(\alpha_3)\frac{1}{H_\gamma^{-}}\frac{\partial \mathbf{v}^{-}}{\partial\alpha_\gamma}+N^{+}(\alpha_3)\frac{1}{H_\gamma^{+}}\frac{\partial \mathbf{v}^{+}}{\partial\alpha_\gamma}\right]\mathbf{e}_\gamma,\quad \varepsilon_{33}^{b}=0$$

$$\varepsilon_{12}^{b}=\left[N^{-}(\alpha_3)\frac{1}{H_1^{-}}\frac{\partial \mathbf{v}^{-}}{\partial\alpha_1}+N^{+}(\alpha_3)\frac{1}{H_1^{+}}\frac{\partial \mathbf{v}^{+}}{\partial\alpha_1}\right]\mathbf{e}_2+\left[N^{-}(\alpha_3)\frac{1}{H_2^{-}}\frac{\partial \mathbf{v}^{-}}{\partial\alpha_2}+N^{+}(\alpha_3)\frac{1}{H_2^{+}}\frac{\partial \mathbf{v}^{+}}{\partial\alpha_2}\right]\mathbf{e}_1 \tag{4}$$

$$\varepsilon_{\gamma 3}^{b}=\boldsymbol{\beta}\mathbf{e}_\gamma+\frac{1}{\bar{H}_\gamma}\frac{\partial \mathbf{v}}{\partial\alpha_\gamma}\mathbf{e}_3,\quad \boldsymbol{\beta}=\frac{1}{h}(\mathbf{v}^{+}-\mathbf{v}^{-}),\quad \mathbf{v}=\frac{1}{2}(\mathbf{v}^{-}+\mathbf{v}^{+})$$

 

The strain–displacement equations (4) are more attractive than Equations (3) because they are completely free for small rigid body motions. It will be shown in the next section. Besides, tangential strains $\varepsilon^{\mathrm{b}}_{\alpha\beta}$ are distributed over the shell thickness according to the linear law. As can be seen from Figure 2, it is an acceptable assumption for the moderately thick shells because the coupling conditions

$$\varepsilon^{\mathrm{a}}_{\alpha\beta}(\delta^{\pm})=\varepsilon^{\mathrm{b}}_{\alpha\beta}(\delta^{\pm})=E^{\pm}_{\alpha\beta}$$

are valid.

More simple strain–displacement equations can be obtained for the *thin* shells replacing the Lamé coefficients $H_\gamma$ and $\bar{H}_\gamma$ by the Lamé coefficients of the reference surface $A_\gamma$ in formulas (3a) and (3b). As a result we have

$$\begin{aligned}
\varepsilon^{\mathrm{c}}_{\gamma\gamma} &= \left[N^{-}(\alpha_3)\frac{1}{A_\gamma}\frac{\partial \mathbf{v}^{-}}{\partial \alpha_\gamma}+N^{+}(\alpha_3)\frac{1}{A_\gamma}\frac{\partial \mathbf{v}^{+}}{\partial \alpha_\gamma}\right]\mathbf{e}_\gamma, \quad \varepsilon^{\mathrm{c}}_{33}=0\\
\varepsilon^{\mathrm{c}}_{12} &= \left[N^{-}(\alpha_3)\frac{1}{A_1}\frac{\partial \mathbf{v}^{-}}{\partial \alpha_1}+N^{+}(\alpha_3)\frac{1}{A_1}\frac{\partial \mathbf{v}^{+}}{\partial \alpha_1}\right]\mathbf{e}_2\\
&\quad+\left[N^{-}(\alpha_3)\frac{1}{A_2}\frac{\partial \mathbf{v}^{-}}{\partial \alpha_2}+N^{+}(\alpha_3)\frac{1}{A_2}\frac{\partial \mathbf{v}^{+}}{\partial \alpha_2}\right]\mathbf{e}_1\\
\varepsilon^{\mathrm{c}}_{\gamma 3} &= \boldsymbol{\beta}\mathbf{e}_\gamma+\frac{1}{A_\gamma}\frac{\partial \mathbf{v}}{\partial \alpha_\gamma}\mathbf{e}_3, \quad \boldsymbol{\beta}=\frac{1}{h}(\mathbf{v}^{+}-\mathbf{v}^{-}), \quad \mathbf{v}=\frac{1}{2}(\mathbf{v}^{-}+\mathbf{v}^{+})
\end{aligned} \tag{5}$$

As we shall see in the next section, the strain–displacement equations (5) can never be free for small rigid body motions.

## 3. RIGID BODY MOTIONS

A small rigid body motion is defined as [24]

$$\mathbf{u}^{\mathrm{R}}=\boldsymbol{\Delta}+\boldsymbol{\Phi}\times\mathbf{R} \tag{6}$$

where $\boldsymbol{\Delta}=\sum_i \Delta_i\mathbf{e}_i$ is the constant displacement (translation) vector; $\boldsymbol{\Phi}=\sum_i \Phi_i\mathbf{e}_i$ is the constant rotation vector; $\mathbf{R}=\mathbf{r}+\alpha_3\mathbf{e}_3$ is the position vector of any point of the shell; $\mathbf{r}$ is the position vector of any point of the reference surface (see Figure 1). In particular, rigid body motions of the face surfaces are

$$\mathbf{v}^{\pm\mathrm{R}}=\boldsymbol{\Delta}+\boldsymbol{\Phi}\times\mathbf{R}^{\pm} \tag{7}$$

where $\mathbf{R}^{\pm}=\mathbf{r}+\delta^{\pm}\mathbf{e}_3$ are the position vectors of points of the top and bottom surfaces.

The derivatives of the translation and rotation vectors with respect to the reference surface co-ordinates are zero, i.e.

$$\frac{\partial \boldsymbol{\Delta}}{\partial \alpha_\gamma}=\mathbf{0}, \quad \frac{\partial \boldsymbol{\Phi}}{\partial \alpha_\gamma}=\mathbf{0} \tag{8}$$

 

Taking into account the formulas for the derivatives of the unit vectors $\mathbf{e}_i$ along the co-ordinate lines [24] and using Equations (7) and (8), one can obtain the following expressions for the derivatives:

$$\frac{\partial \mathbf{v}^{\pm R}}{\partial \alpha_\gamma} = H_\gamma^{\pm} \boldsymbol{\Phi} \times \mathbf{e}_\gamma \tag{9}$$

It can be verified by using Equations (7) and (9) that the strains given by Equations (4) are all zero in a general rigid body motion, i.e.

$$\varepsilon_{\alpha\alpha}^{bR} = (\boldsymbol{\Phi} \times \mathbf{e}_\alpha)\mathbf{e}_\alpha = 0, \quad \varepsilon_{ij}^{bR} = 0 \quad (i \neq j)$$

So, the TM theory of moderately thick shells is completely strain-free for all rigid body motions.

Using again Equations (7) and (9) in the strain–displacement equations (5), we get the following results:

$$\varepsilon_{\alpha\alpha}^{cR} = (1 + k_\alpha \alpha_3)(\boldsymbol{\Phi} \times \mathbf{e}_\alpha)\mathbf{e}_\alpha = 0, \quad \varepsilon_{12}^{cR} = (k_1 - k_2)\alpha_3(\boldsymbol{\Phi} \times \mathbf{e}_1)\mathbf{e}_2$$

$$\varepsilon_{\alpha 3}^{cR} = k_\alpha \bar{\delta}(\boldsymbol{\Phi} \times \mathbf{e}_\alpha)\mathbf{e}_3$$

showing that rigid body motions can never be completely strain free for the TM theory of thin shells. However, the transverse shear strains $\varepsilon_{\alpha 3}^{cR} = 0$ when a reference surface is selected to be the middle surface, since in this case $\bar{\delta} = 0$. The tangential shear strain $\varepsilon_{12}^{cR} = 0$ in the case of spherical shells or symmetrically loaded and supported isotropic or orthotropic shells of revolution, and at the reference surface points of anisotropic shells of arbitrary geometry.

## 4. HU–WASHIZU FUNCTIONAL

Let us consider the shell built up in the general case by the arbitrary superposition across the wall thickness of $N$ thin layers of uniform thickness $h_k$. The $k$th layer may be defined as a three-dimensional body of volume $V_k$ bounded by two surfaces $S_{k-1}$ and $S_k$, located at the distances $\delta_{k-1}$ and $\delta_k$ measured with respect to the reference surface $S$, and the edge boundary surface $\Omega_k$ that is perpendicular to the reference surface (see Figure 3). Here and in the following developments the index $k = \overline{1,N}$ identifies the belonging of any quantity to the $k$th layer. The full edge boundary surface $\Omega = \Omega_1 + \Omega_2 + \cdots + \Omega_N$ is generated by the normals to the reference surface along the bounding curve $\Gamma$ (with the arc length $s$) of this surface. It is also assumed that the bounding surfaces $S_{k-1}$ and $S_k$ are continuous, sufficiently smooth and without any singularities. Let the reference surface be referred to an orthogonal curvilinear co-ordinate system $\alpha_1$ and $\alpha_2$ which coincides with the lines of principal curvatures of its surface. The $\alpha_3$ axis is oriented along the outward unit vector $\mathbf{e}_3$ normal to the reference surface.

The constituent layers of the shell are supposed to be rigidly joined, so that no slip on contact surfaces and no separation of layers can occur. The material of each constituent layer is assumed to be linearly elastic, anisotropic, homogeneous or fibre reinforced, such that in each point there is a single surface of elastic symmetry parallel to the reference surface. Let $p_i^-$

 

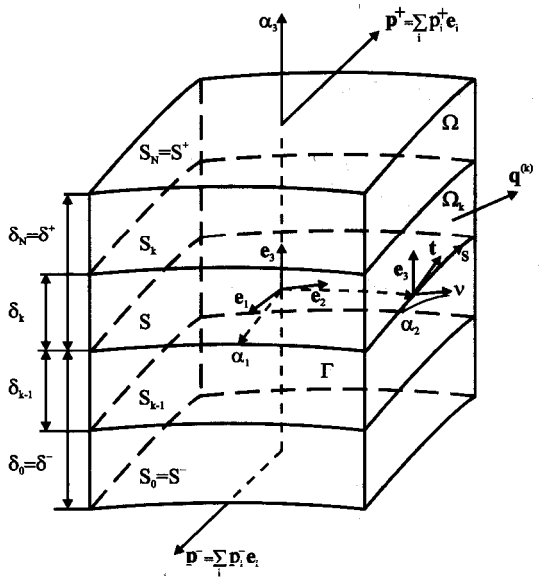


Figure 3. Multilayered shell element.

and $p_i^+$ be the intensities of the external loading acting on the bottom surface $S^-=S_0$ and top surface $S^+=S_N$ in the $\alpha_i$ co-ordinate directions, respectively, while $\mathbf{q}^{(k)}=q_\nu^{(k)}\mathbf{v}+q_t^{(k)}\mathbf{t}+q_3^{(k)}\mathbf{e}_3$ be the external loading vector acting on the edge boundary surface $\Omega_k$. Here, $q_\nu^{(k)}$, $q_t^{(k)}$ and $q_3^{(k)}$ are the components of its vector acting in the $\nu$, $t$ and $\alpha_3$ directions; $\mathbf{v}$ and $\mathbf{t}$ are the normal and tangential unit vectors to the bounding curve $\Gamma$.

The refined TM theory of multilayered shells is also based on the linear approximation of the displacement vector in the thickness direction (2), where we should set $\delta^-=\delta_0$ and $\delta^+=\delta_N$. Substituting the displacements (2) and strains rewritten in the more convenient form

$$\varepsilon_{\alpha\beta}=N^-(\alpha_3)E_{\alpha\beta}^-+N^+(\alpha_3)E_{\alpha\beta}^+,\quad \varepsilon_{\alpha3}=E_{\alpha3},\quad \varepsilon_{33}=0 \tag{10}$$

into the Hu–Washizu functional [3, 25] and taking into account the strain–displacement relationships (4) for the moderately thick shell, one can obtain

$$\begin{aligned} J=\iint_S \Bigg\{ &\Pi-\sum_{\alpha\leqslant\beta}[R_{\alpha\beta}^-(E_{\alpha\beta}^- - e_{\alpha\beta}^-)+R_{\alpha\beta}^+(E_{\alpha\beta}^+ - e_{\alpha\beta}^+)] \\ &-\sum_\alpha [R_{\alpha3}(E_{\alpha3}-e_{\alpha3})+(Q_\alpha^- - p_\alpha^-)v_\alpha^- +(Q_\alpha^+ + p_\alpha^+)v_\alpha^+]-(Q_3 - p_3^- + p_3^+)v_3 \Bigg\}\,\mathrm{d}S \\ &-\oint_\Gamma (\hat{R}_{\nu\nu}^- v_\nu^- + \hat{R}_{\nu\nu}^+ v_\nu^+ + \hat{R}_{\nu t}^- v_t^- + \hat{R}_{\nu t}^+ v_t^+ + \hat{R}_{\nu3}v_3)\,\mathrm{d}s \end{aligned} \tag{11}$$

 

where

$$
\begin{aligned}
&e_{\gamma\gamma}^{\pm}=\frac{1}{\zeta_{\gamma}^{\pm}}\left(\frac{1}{A_{\gamma}}\frac{\partial v_{\gamma}^{\pm}}{\partial\alpha_{\gamma}}+B_{\delta}v_{\delta}^{\pm}+k_{\gamma}v_{3}\right)\\
&e_{12}^{\pm}=\frac{1}{\zeta_{1}^{\pm}}\left(\frac{1}{A_{1}}\frac{\partial v_{2}^{\pm}}{\partial\alpha_{1}}-B_{2}v_{1}^{\pm}\right)+\frac{1}{\zeta_{2}^{\pm}}\left(\frac{1}{A_{2}}\frac{\partial v_{1}^{\pm}}{\partial\alpha_{2}}-B_{1}v_{2}^{\pm}\right),\quad e_{\gamma 3}=\beta_{\gamma}-\frac{1}{\bar{\zeta}_{\gamma}}\theta_{\gamma}\\
&\theta_{\gamma}=k_{\gamma}v_{\gamma}-\frac{1}{A_{\gamma}}\frac{\partial v_{3}}{\partial\alpha_{\gamma}},\quad \beta_{\gamma}=\frac{1}{h}(v_{\gamma}^{+}-v_{\gamma}^{-}),\quad v_{\gamma}=\frac{1}{2}(v_{\gamma}^{-}+v_{\gamma}^{+})\\
&\zeta_{\gamma}^{\pm}=1+k_{\gamma}\delta^{\pm},\quad \bar{\zeta}_{\gamma}=1+k_{\gamma}\bar{\delta},\quad B_{\gamma}=\frac{1}{A_{1}A_{2}}\frac{\partial A_{\delta}}{\partial\alpha_{\gamma}}\quad(\delta\neq\gamma)
\end{aligned}
\tag{12}
$$

Here, $\Pi$ is the strain energy density; $v_{v}^{\pm}$, $v_{t}^{\pm}$ and $v_3$ are the components of the displacement vectors of the face surfaces in the co-ordinate system $v$, $t$ and $\alpha_3$ (see Figure 3); $E_{\alpha\beta}^{\pm}$ are the tangential strains of the bottom and top surfaces; $E_{\alpha 3}$ are the transverse shear strains of the middle surface; $R_{\alpha\beta}^{\pm}$ and $R_{\alpha 3}$ are the generalized and classical stress resultants; $Q_{\alpha}^{\pm}$ and $Q_3$ are the generalized and classical body force resultants; $\hat{R}_{vv}^{\pm}$, $\hat{R}_{vt}^{\pm}$ and $\hat{R}_{v3}$ are the generalized and classical external load resultants, which are defined as

$$
\begin{aligned}
\Pi=&\frac{1}{2}\sum_{\alpha\leqslant\beta}\sum_{\gamma\leqslant\delta}[A_{\alpha\beta\gamma\delta}^{00}E_{\alpha\beta}^{-}E_{\gamma\delta}^{-}+A_{\alpha\beta\gamma\delta}^{01}(E_{\alpha\beta}^{-}E_{\gamma\delta}^{+}+E_{\alpha\beta}^{+}E_{\gamma\delta}^{-})+A_{\alpha\beta\gamma\delta}^{11}E_{\alpha\beta}^{+}E_{\gamma\delta}^{+}]\\
&+\frac{1}{2}\sum_{\alpha,\gamma}A_{\alpha 3\gamma 3}E_{\alpha 3}E_{\gamma 3},\quad A_{\alpha 3\gamma 3}=\sum_{k}\int_{\delta_{k-1}}^{\delta_{k}}C_{\alpha 3\gamma 3}^{(k)}\,\mathrm{d}\alpha_{3}\\
A_{\alpha\beta\gamma\delta}^{mn}=&\sum_{k}\int_{\delta_{k-1}}^{\delta_{k}}C_{\alpha\beta\gamma\delta}^{(k)}[N^{-}(\alpha_{3})]^{2-m-n}[N^{+}(\alpha_{3})]^{m+n}\,\mathrm{d}\alpha_{3}\quad(m,n=0,1)
\end{aligned}
\tag{13}
$$

and

$$
\begin{aligned}
&R_{\alpha\beta}^{\pm}=\sum_{k}\int_{\delta_{k-1}}^{\delta_{k}}\sigma_{\alpha\beta}^{(k)}N^{\pm}(\alpha_{3})\,\mathrm{d}\alpha_{3},\quad R_{\alpha 3}=\sum_{k}\int_{\delta_{k-1}}^{\delta_{k}}\sigma_{\alpha 3}^{(k)}\mathrm{d}\alpha_{3}\\
&Q_{\alpha}^{\pm}=\sum_{k}\int_{\delta_{k-1}}^{\delta_{k}}f_{\alpha}^{(k)}N^{\pm}(\alpha_{3})\,\mathrm{d}\alpha_{3},\quad Q_{3}=\sum_{k}\int_{\delta_{k-1}}^{\delta_{k}}f_{3}^{(k)}\,\mathrm{d}\alpha_{3}\\
&\hat{R}_{vv}^{\pm}=\sum_{k}\int_{\delta_{k-1}}^{\delta_{k}}q_{v}^{(k)}N^{\pm}(\alpha_{3})\,\mathrm{d}\alpha_{3},\quad \hat{R}_{vt}^{\pm}=\sum_{k}\int_{\delta_{k-1}}^{\delta_{k}}q_{t}^{(k)}N^{\pm}(\alpha_{3})\,\mathrm{d}\alpha_{3}\\
&\hat{R}_{v3}=\sum_{k}\int_{\delta_{k-1}}^{\delta_{k}}q_{3}^{(k)}\,\mathrm{d}\alpha_{3}
\end{aligned}
\tag{14}
$$

In formulas (14) $f_{\alpha}^{(k)}$ and $f_{3}^{(k)}$ are the externally applied body forces of the $k$th layer, while $\sigma_{\alpha\beta}^{(k)}$ and $\sigma_{\alpha 3}^{(k)}$ denote the tangential and transverse shear stresses of the $k$th layer that can be

 

found as

$$\sigma_{\alpha\beta}^{(k)}=\sum_{\gamma\leqslant\delta} C_{\alpha\beta\gamma\delta}^{(k)}\varepsilon_{\gamma\delta},\quad \sigma_{\alpha 3}^{(k)}=\sum_{\gamma} C_{\alpha 3\gamma 3}^{(k)}\varepsilon_{\gamma 3}$$

where $C_{\alpha\beta\gamma\delta}^{(k)}$ and $C_{\alpha 3\gamma 3}^{(k)}$ are the stiffness coefficients of the $k$th layer.

## 5. FE FORMULATION

It is well known that the Hu–Washizu variational principle provides the basis for the derivation of various variational principles, and many different mixed and hybrid finite elements can be designed [26]. Herein, the Hu–Washizu functional (11)–(14) for the element can be written in the following form:

$$J^{\mathrm{el}}=\int_{-1}^{1}\int_{-1}^{1}\left[\tfrac{1}{2}\mathbf{E}^{\mathrm{T}}\mathbf{A}\mathbf{E}-(\mathbf{E}^{\mathrm{T}}-\mathbf{v}^{\mathrm{T}}\mathbf{B}^{\mathrm{T}})\mathbf{R}-\mathbf{v}^{\mathrm{T}}(\mathbf{P}+\mathbf{Q})\right]\Lambda\,\mathrm{d}\xi_1\,\mathrm{d}\xi_2-\oint_{\Gamma^{\mathrm{el}}}\mathbf{v}_\Gamma^{\mathrm{T}}\hat{\mathbf{R}}_\Gamma\,\mathrm{d}s \tag{15}$$

where $\xi_1$ and $\xi_2$ are the local co-ordinates of the element that vary from $-1$ to $+1$; $\Lambda(\xi_1,\xi_2)$ is the function characterizing the metric of the element; $v=[v_1^-\ v_1^+\ v_2^-\ v_2^+\ v_3]^{\mathrm{T}}$ is the displacement vector; $\mathbf{v}_\Gamma=[v_v^-\ v_v^+\ v_t^-\ v_t^+\ v_3]^{\mathrm{T}}$ is the displacement vector of the element edge $\Gamma^{\mathrm{el}}$; $\mathbf{E}=[E_{11}^-\ E_{11}^+\ E_{22}^-\ E_{22}^+\ E_{12}^-\ E_{12}^+\ E_{13}\ E_{23}]^{\mathrm{T}}$ is the strain vector; $\mathbf{R}=[R_{11}^-\ R_{11}^+\ R_{22}^-\ R_{22}^+\ R_{12}^-\ R_{12}^+\ R_{13}\ R_{23}]^{\mathrm{T}}$ is the stress resultant vector; $\hat{\mathbf{R}}_\Gamma=[\hat{R}_{vv}^-\ \hat{R}_{vv}^+\ \hat{R}_{vt}^-\ \hat{R}_{vt}^+\ R_{v3}]^{\mathrm{T}}$ is the loading resultant vector acting on the element edge $\Gamma^{\mathrm{el}}$; $\mathbf{Q}=[Q_1^-\ Q_1^+\ Q_2^-\ Q_2^+\ Q_3]^{\mathrm{T}}$ is the body force resultant vector; $\mathbf{P}=[-p_1^-\ p_1^+-p_2^-\ p_2^+-p_3^-+p_3^+]^{\mathrm{T}}$ is the surface traction vector; $\mathbf{A}$ is the constitutive stiffness matrix; $\mathbf{B}$ is the strain–displacement matrix.

For the quadrilateral 4-node shell element the displacement field is approximated according to the standard $C^0$ interpolation:

$$\mathbf{v}=\sum_{\mathrm{l}} N_{\mathrm{l}}\mathbf{v}_{\mathrm{l}} \tag{16}$$

where $\mathbf{v}_\ell=[v_{1\ell}^-\ v_{1\ell}^+\ v_{2\ell}^-\ v_{2\ell}^+\ v_{3\ell}]^{\mathrm{T}}$ are the displacement vectors of the element nodes; $N_\ell(\xi_1,\xi_2)$ are the linear shape functions of the element; $\ell=\overline{1,4}$.

In accordance with [22, 23], the 20 modes of this element are the six rigid body motions, the eight homogeneous states of strains $E_{\alpha\beta}^{-00}$, $E_{\alpha\beta}^{+00}$, $E_{\alpha 3}^{00}$, and the six additional modes representing higher approximations of tangential normal strains $E_{11}^{-01}$, $E_{11}^{+01}$, $E_{22}^{-10}$, $E_{22}^{+10}$ and transverse shear strains $E_{13}^{01}$, $E_{23}^{10}$, i.e. we have following strain interpolations:

$$\begin{aligned}
&\mathbf{E}=\mathbf{E}^{00}+\mathbf{E}^{10}\xi_1+\mathbf{E}^{01}\xi_2\\
&\mathbf{E}^{00}=[E_{11}^{-00}\ E_{11}^{+00}\ E_{22}^{-00}\ E_{22}^{+00}\ E_{12}^{-00}\ E_{12}^{+00}\ E_{13}^{00}\ E_{23}^{00}]^{\mathrm{T}}\\
&\mathbf{E}^{01}=[E_{11}^{-01}\ E_{11}^{+01}\ 0\ 0\ 0\ 0\ E_{13}^{01}\ 0]^{\mathrm{T}},\quad E^{10}=[0\ 0\ E_{22}^{-10}\ E_{22}^{+10}\ 0\ 0\ 0\ E_{23}^{10}]^{\mathrm{T}}
\end{aligned} \tag{17}$$

The interpolations of the stress resultants follow the forms of the conjugate strains

$$\mathbf{R}=\mathbf{R}^{00}+\mathbf{R}^{10}\xi_1+\mathbf{R}^{01}\xi_2 \tag{18}$$

 

where the vectors $\mathbf{R}^{00}$, $\mathbf{R}^{01}$ and $\mathbf{R}^{10}$ are defined from Equations (17) by replacing a letter $E$ by a letter $R$.

The governing equations for the element are obtained by applying the Hu–Washizu variational principle (15). Using Equations (16)–(18), and eliminating the strain and stress resultant parameters on the element level, one can obtain

$$\mathbf{Ku}=\mathbf{F}$$

where $\mathbf{K}$ is the elemental stiffness matrix; $\mathbf{F}$ is the load vector; $\mathbf{u}$ is the vector of five displacement components at nodal points of the element.

It should be noted that the formulation of the stiffness matrix $\mathbf{K}$ requires only direct substitutions; no inversion is needed if the element is rectangular. The matrix is symmetric and positive definite, and has six, and only six, zero eigenvalues as required for satisfaction of the general rigid body motion representation. Furthermore, the element matrix is evaluated by using the full exact analytical integration and the element does not contain any spurious zero energy modes. So, our FE formulation especially for the rectangular elements is very economical and efficient.

## 6. NUMERICAL TESTS

Four tests were employed to assess the effectiveness of the developed TMS4 element based on the strain–displacement equations (4) that are completely free for all rigid body motions. They were a pinched cylinder with rigid end-diaphragms, a pinched cylinder with free edges, a cylindrical shell roof, and a multilayered angle-ply cylindrical shell.

### *6.1. Pinched cylinder with rigid diaphragms*

To illustrate the capability of the developed TMS4 element to overcome membrane and shear locking phenomenon and to compare it with the different 4-node quadrilateral elements [15, 16, 18, 27, 28], we consider one of the most demanding standard linear tests [29]. A thin cylinder supported by rigid end-diaphragms is loaded by two opposite concentrated forces in its middle section. The geometrical and material data of the problem are shown in Figure 4(a). Three types of boundary conditions modelling the rigid end-diaphragm can be used:

$$v_2^- = v_3 = 0 \tag{19a}$$

$$v_2^+ = v_3 = 0 \tag{19b}$$

$$v_2^- = v_2^+ = v_3 = 0 \tag{19c}$$

Besides, due to symmetry of the problem, only one octant of the cylinder is modelled with a regular mesh of TMS4 elements.

Table I lists a comparison of the normalized radial displacement under the applied load between the TMS4 element and aforementioned 4-node quadrilateral elements [30]. The displacements are normalized with respect to the analytical solution $-1.8245 \times 10^{-5}$ [29].

 

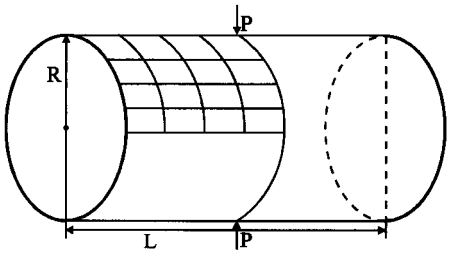


(a) Rigid diaphragms: R=300, L=600, h=3
E=3×10$^6$, ν=0.3, P=1
(b) Free edges: R=4.953, L=10.35, h=0.094
E=1.05×10$^7$, ν=0.3125, P=100

Figure 4. Pinched cylinder under opposite radial forces with: (a) rigid diaphragms and; (b) free edges.

Table I. Pinched cylinder with rigid diaphragms. Normalized radial displacement under the concentrated load.

| Mesh | MITC4 [15] | RSDS [16] | Mixed [18] | SRI [27] | QPH [28] | TMS4 (19a) | TMS4 (19c) |
|---|---|---|---|---|---|---|---|
| 4 × 4 | 0.370 | 0.469 | 0.399 | 0.373 | 0.370 | 0.890 | 0.890 |
| 8 × 8 | 0.740 | 0.791 | 0.763 | 0.747 | 0.740 | 0.941 | 0.941 |
| 16 × 16 | 0.930 | 0.946 | 0.935 | 0.935 | 0.930 | 0.986 | 0.986 |

Note that all the three variants of boundary conditions (19) lead to the practically identical results and very well model the 'real' boundary conditions,

$$v_2 = v_3 = 0 \tag{20}$$

used by Heppler and Hansen [29]. As can be seen from Table I, our results show an excellent agreement even for coarse meshes.

### 6.2. *Pinched cylinder with free edges*

The pinched cylinder with free edges has been also extensively treated for numerical testing of new FE models. The geometrical and material properties of the cylinder are shown in Figure 4(b). Owing to symmetry of the problem, only one octant of the cylinder is discretized. The radial deflection at the load is given in Figure 5. The curves marked by • display the results obtained by using the TMS4 element. Additionally, in Figure 5 the solutions, based on the traditional cubic Lagrange element [31] (see curves marked by ♦) and the cubic Lagrange element [31] that has been augmented in the manner of Cantin [32] to provide the correct rigid body motions (see curves marked by ▲), are presented. Both the Lagrange elements are based on the classical TM shell theory. Note that the augmented Lagrange element solution converges to value −0.1114 [31] as do the developed TMS4 element and the cubic Lagrange element. However, our simple and efficient element solution converges more rapidly, since the cubic Lagrange element possesses only two zero eigenvalues. At the same time its augmented

 

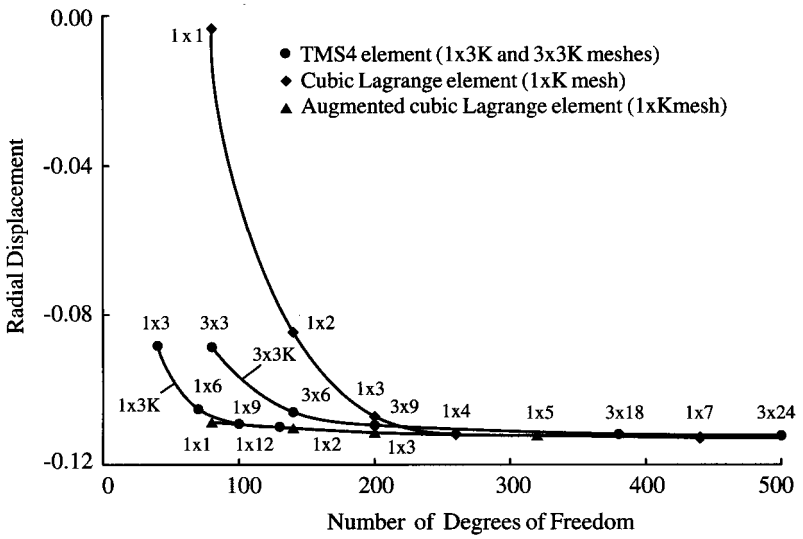


Figure 5. Pinched cylinder with free edges. Radial displacement under load.

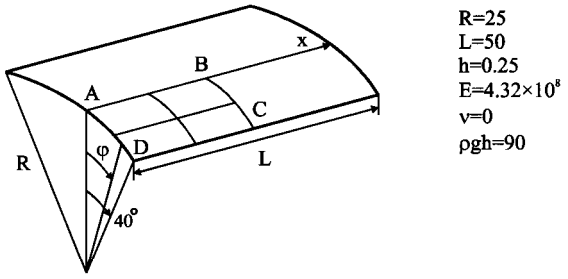


Figure 6. Cylindrical shell roof under self-weight loading.

formulation has the six zero eigenvalues as required for satisfaction of the general rigid body motion requirements.

### *6.3. Cylindrical shell roof*

Let us consider an open cylindrical shell segment subjected to gravitational self-weight loading and supported at its curved edges by rigid diaphragms, while the straight edges are free [33]. This problem has become a de facto standard test and has been frequently used for numerical testing of FE approximations. The geometrical and material characteristics of the shell are depicted in Figure 6. Owing to symmetry of the problem, only one quarter of the roof is modelled with a regular mesh of TMS4 elements. Figure 7 shows the distribution of the axial displacement at the diaphragm (around the curve AD) and the vertical displacement at the middle span (around the curve BC), while Figure 8 displays the distribution of the moment resultants $M_{\alpha\alpha}=h(R^{+}_{\alpha\alpha}-R^{-}_{\alpha\alpha})/2$ at the middle span. The solid curves show the results obtained by using the exact solution [33] as reported in works [11, 12]. One can see that the moment

 

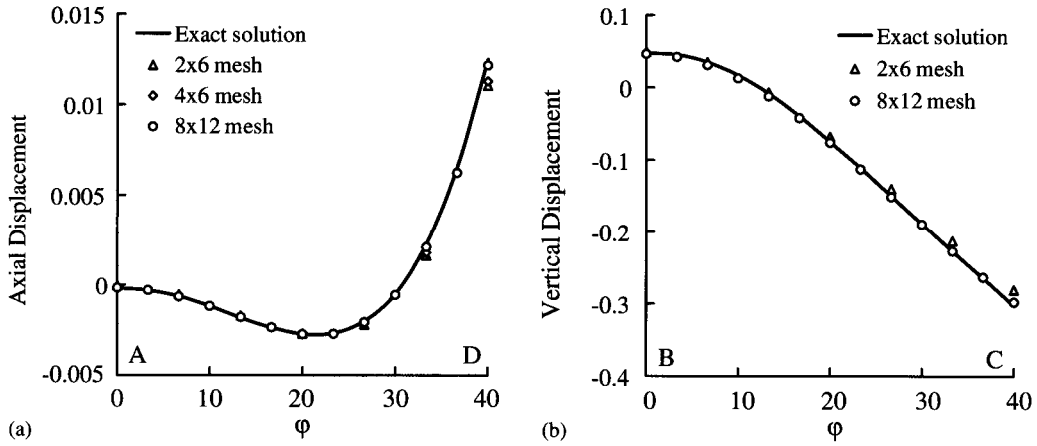


Figure 7. Cylindrical shell roof. Displacements: at (a) diaphragm and; (b) middle span.

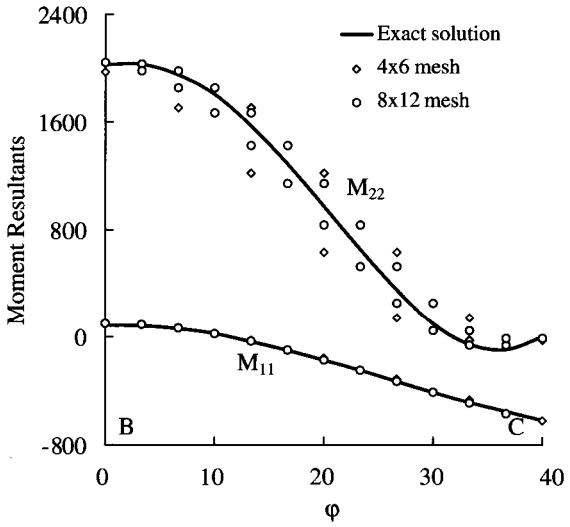


Figure 8. Cylindrical shell roof. Moment resultants at middle span.

resultant $M_{11}$ is calculated with an excellent exactitude for both meshes. However, the results obtained for the moment resultant $M_{22}$ are less satisfactory. This phenomenon is explained by using the constant approximation over the element for generalized stress resultants $R_{22}^{\pm}$ in $\varphi$ direction in accordance with Equations (18).

Table II additionally presents a comparison of the normalized vertical displacement at the point $C$ of the middle span between the TMS4 element and aforementioned 4-node quadrilateral elements [15, 18, 27, 28]. The displacements [30] are normalized to the value $-0.3024$ calculated by MacNeal and Harder [34], while our displacement is normalized to the value

 

Table II. Cylindrical shell roof. Normalized vertical displacement at point C (see Figure 6).

| Mesh | MITC4 [15] | Mixed [18] | SRI [27] | QPH [28] | TMS4 |
|---|---|---|---|---|---|
| 4 × 4 | 0.940 | 1.083 | 0.964 | 0.940 | 0.864 |
| 8 × 8 | 0.970 | 1.015 | 0.984 | 0.980 | 0.962 |
| 16 × 16 | 1.000 | 1.000 | 0.999 | 1.010 | 0.989 |

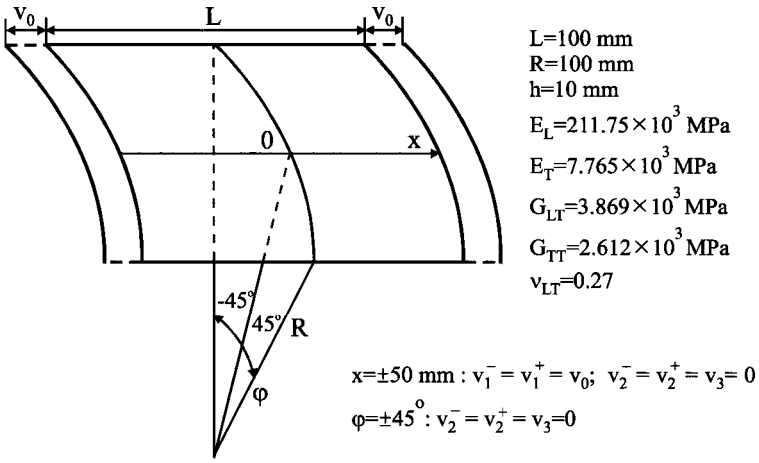


Figure 9. Two-layer angle-ply cylindrical shell subjected to uniform stretching.

−0.3015. Such a value is a computationally exact solution of this problem based on the developed TM shell theory. The slightly small difference between the reference solutions is explained by a simple fact: in this test the shell response is more sensitive to the types of boundary conditions modelling the rigid end-diaphragm (see for the comparison a pinched cylinder with rigid diaphragms). One can observe that boundary conditions (19c) used in our FE formulation provide the more rigid end support than (20) used in works [33, 34].

### 6.4. *Multilayered angle-ply cylindrical shell*

It is apparent that using the simplified strain–displacement equations (5) can lead to incorrect results for the moderately thick composite shells. To assess this statement, we consider an open cylindrical two-layer angle-ply shell rigidly clamped at its curved edges and supported at straight edges by rigid diaphragms. The shell is subjected to the uniform stretching $v_0$ as shown in Figure 9. The material characteristics of each layer were taken to be those typical of a high modulus composite [7] and are given in Figure 9, where subscripts L and T refer to the longitudinal and transverse directions of the individual ply. Let the ply thicknesses and ply orientations be $[h/2, h/2]$ and $[-\gamma, +\gamma]$, where $\gamma$ is measured in the clockwise direction from $x$ to the fibre direction. Due to the anisotropic shell response, we did not adopt symmetry conditions and modelled the whole shell by using regular meshes of TMS4 and TMS4c elements. The newly developed TMS4c element is based on the simplified strain–displacement equations (5).

 

Table III. Central transverse displacement $-v_3(0,0)/v_0$ of the two-layer angle-ply cylindrical shell.

| | TMS4 | | | | TMS4c | | | |
|---|---|---|---|---|---|---|---|---|
| Mesh | [0°,90°] | [−15°,15°] | [−30°,30°] | [−60°,60°] | [0°,90°] | [−15°,15°] | [−30°,30°] | [−60°,60°] |
| 4 × 4 | 0.077 | 1.705 | 4.091 | 1.469 | 0.077 | 1.703 | 4.085 | 1.468 |
| 4 × 8 | 0.068 | 1.346 | 3.359 | 1.259 | 0.067 | 1.344 | 3.352 | 1.259 |
| 4 × 12 | 0.066 | 1.330 | 3.301 | 1.219 | 0.066 | 1.329 | 3.295 | 1.219 |
| 8 × 8 | 0.065 | 1.439 | 3.501 | 1.182 | 0.064 | 1.437 | 3.493 | 1.181 |
| 8 × 16 | 0.063 | 1.413 | 3.418 | 1.126 | 0.062 | 1.412 | 3.411 | 1.126 |
| 8 × 24 | 0.063 | 1.409 | 3.404 | 1.116 | 0.062 | 1.407 | 3.398 | 1.115 |
| 12 × 12 | 0.063 | 1.434 | 3.456 | 1.131 | 0.062 | 1.433 | 3.449 | 1.131 |
| 12 × 24 | 0.062 | 1.423 | 3.422 | 1.106 | 0.062 | 1.422 | 3.416 | 1.105 |

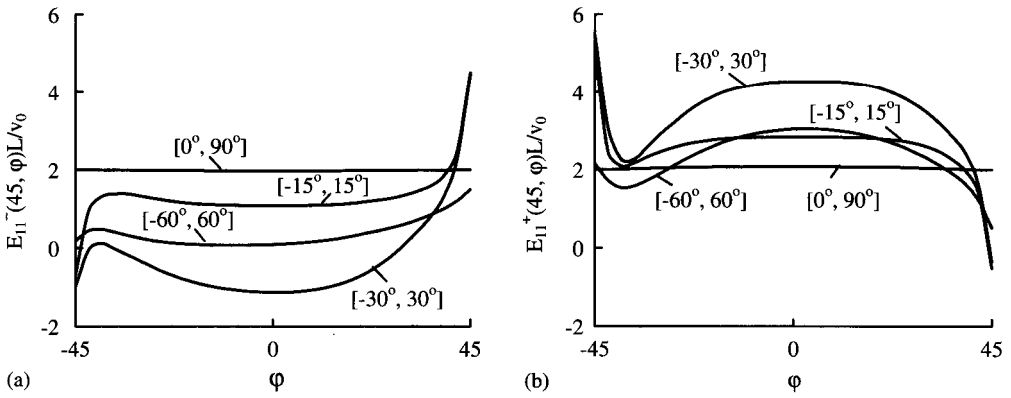


Figure 10. Distribution of longitudinal strains of bottom and top surfaces: (a) $E_{11}^{-}$; and (b) $E_{11}^{+}$ at $x=45$ mm in $\varphi$ direction.

In Table III the values of the dimensionless central transverse displacement of the shell segment for both TMS4 and TMS4c elements and for various ply orientations and meshes are presented. It can be seen that using the strain–displacement equations (4) only insignificantly updates the results in a comparison with less general strain–displacement equations (5). Thus, it is possible to recommend the geometrically linear TM shell theory on the basis of strain–displacement equations (5) for using in engineering calculations. At the same time applying the TM shell theory, which is not completely strain-free for rigid body motions for solving the composite shells undergoing large deflections and large rotations can lead to significant errors. Such a problem is currently under development. Finally, Figure 10 shows the distribution of the longitudinal strains of the face surfaces at $x=45$ mm in $\varphi$ direction for various ply orientations. It is seen that a response of the shell is very unusual to the ply orientation [−30°,30°], where the longitudinal strain of the bottom surface is negative.

 

## 7. CONCLUSION

The simple and efficient mixed models have been developed for the analysis of multilayered anisotropic TM shells. The first FE formulation is based on the strain–displacement equations of the *moderately thick* shell, which are completely free for rigid body motions. The second FE formulation is based on the strain–displacement equations of the *thin* shell that cannot be completely free for rigid body motions in the case of anisotropic shells of arbitrary geometry. As fundamental unknowns five displacements and eight strains of the face surfaces of the shell, and eight stress resultants have been chosen. This allows, in particular, special loading conditions at the bottom and top surfaces of the shell to be accounted for.

The elemental stiffness matrices of our FE formulations are symmetric and positive definite and have six zero eigenvalues as required for satisfaction of the general rigid body motion representation. Besides, the elemental matrices require only direct substitutions (no inversion is needed) if elements are rectangular and they are evaluated using the full exact analytical integration. It is important that the developed TMS4 and TMS4c elements do not contain any spurious zero energy modes.

To demonstrate the high accuracy and effectiveness of the developed elements four tests were employed. They were pinch tests, an open cylindrical shell roof test and an open cylindrical composite shell test.

The extension to finite deflections poses no additional difficulties but requires algebra and computation efforts. For this purpose the Hu–Washizu mixed functional for an analysis of geometrically non-linear multilayered anisotropic shells [3, 25] can be used. The extension to initially stressed multilayered shells can also be done [35].

ACKNOWLEDGEMENTS

The present research was supported by the Russian Fund of Basic Research (Grant No. 98-01-04076) and by the Research Programme of Tambov State Technical University (Grant No. 1Г/00-10).

REFERENCES

1. Cantin G. Strain displacement relationships for cylindrical shells. *AIAA Journal* 1968; **6**:1787–1788.
2. Dawe DJ. Rigid-body motions and strain-displacement equations of curved shell finite elements. *International Journal of Mechanical Sciences* 1972; **14**:569–578.
3. Kulikov GM, Plotnikova SV. Comparative analysis of two algorithms for numerical solution of non-linear static problems for multilayered anisotropic shells of revolution. 1. Account of transverse shear. *Mechanics of Composite Materials* 1999; **35**:241–248.
4. Kulikov GM. Refined global approximation theory of multilayered plates and shells. *Journal of Engineering Mechanics* (ASCE) 2001; **127**:119–125.
5. Timoshenko SP. On the correction for shear of the differential equation for transverse vibrations of prismatic bars. *Philosophical Magazine and Journal of Science. Series 6* 1921; **41**:744–746.
6. Mindlin RD. Influence of rotatory inertia and shear on flexural motions of isotropic elastic plates. *Journal of Applied Mechanics* (ASME) 1951; **18**:31–38.
7. Grigolyuk EI, Kulikov GM. *Multilayered Reinforced Shells: Analysis of Pneumatic Tires*. Mashinostroyenie: Moscow, 1988 (in Russian).
8. Noor AK, Burton WS. Assessment of computational models for multilayered composite shells. *Applied Mechanics Reviews* (ASME) 1990; **43**:67–97.
9. Reddy JN. *Mechanics of Laminated Composite Plates: Theory and Analysis*. CRC Press: Boca Raton, 1997.
10. Kulikov GM, Plotnikova SV. Finite element formulation of straight composite beams undergoing finite rotations. *Transactions of the Tambov State Technical University* 2001; **7**:617–633.
11. Ahmad S, Irons BM, Zienkiewicz OC. Analysis of thick and thin shell structures by curved finite elements. *International Journal for Numerical Methods in Engineering* 1970; **2**:419–451.

 

12. Zienkiewicz OC, Taylor RL, Too JM. Reduced integration technique in general analysis of plates and shells. *International Journal for Numerical Methods in Engineering* 1971; **3**:275–290.
13. Hughes TJR, Taylor RL, Kanok-Nukulchai W. A simple and efficient finite element for plate bending. *International Journal for Numerical Methods in Engineering* 1977; **11**:1529–1543.
14. Malkus DS, Hughes TJR. Mixed finite element methods—reduced and selective integration techniques: a unification of concepts. *Computer Methods in Applied Mechanics and Engineering* 1978; **15**:63–81.
15. Bathe KJ, Dvorkin EN. A formulation of general shell elements—the use of mixed interpolation of tensorial components. *International Journal for Numerical Methods in Engineering* 1986; **22**:697–722.
16. Lam D, Liu WK, Law ES, Belytschko T. Resultant-stress degenerated-shell element. *Computer Methods in Applied Mechanics and Engineering* 1986; **55**:259–300.
17. Stolarski H, Belytschko T. On the equivalence of mode decomposition and mixed finite elements based on the Hellinger–Reissner principle. Part I: Theory. Part II: Applications. *Computer Methods in Applied Mechanics and Engineering* 1986; **58**:249–284.
18. Simo JC, Fox DD, Rifai MS. On a stress resultant geometrically exact shell model. Part II: The linear theory; computational aspects. *Computer Methods in Applied Mechanics and Engineering* 1989; **73**:53–92.
19. Park HC, Cho C, Lee SW. An efficient assumed strain element model with six DOF per node for geometrically non-linear shell. *International Journal for Numerical Methods in Engineering* 1995; **38**:4101–4122.
20. Klinkel S, Gruttmann F, Wagner W. A continuum based three-dimensional shell element for laminated structures. *Computers and Structures* 1999; **71**:43–62.
21. Bathe KJ. *Finite Element Procedures*. Prentice-Hall: New Jersey, 1996.
22. Hughes TJR, Tezduyar TE. Finite elements based upon Mindlin plate theory with particular reference to the four-node bilinear isoparametric element. *Journal of Applied Mechanics* (ASME) 1981; **48**:587–596.
23. Wempner G, Talaslidis D, Hwang CM. A simple and efficient approximation of shells via finite quadrilateral elements. *Journal of Applied Mechanics* (ASME) 1982; **49**:115–120.
24. Gol'denveiser AL. *Theory of Elastic Thin Shell*. Pergamon Press: Oxford, 1961.
25. Kulikov GM. Variational equation for the non-linear multilayered anisotropic shell of variable stiffness. *Transactions of the Tambov State Technical University* 1997; **3**:119–125.
26. Pian THH, Tong P. Basis of finite element methods for solid continua. *International Journal for Numerical Methods in Engineering* 1969; **1**:3–28.
27. Hughes TJR, Liu WK. Nonlinear finite element analysis of shells. Part II: Two-dimensional shells. *Computer Methods in Applied Mechanics and Engineering* 1981; **27**:167–182.
28. Belytschko T, Leviathan I. Physical stabilization of the 4-node shell element with one-point quadrature. *Computer Methods in Applied Mechanics and Engineering* 1994; **113**:321–350.
29. Heppler GR, Hansen JS. A Mindlin element for thick and deep shells. *Computer Methods in Applied Mechanics and Engineering* 1986; **54**:21–47.
30. Argyris JH, Papadrakakis M, Apostolopoulou C, Koutsourelakis S. The TRIC shell element: theoretical and numerical investigation. *Computer Methods in Applied Mechanics and Engineering* 2000; **182**:217–245.
31. Hansen JS, Heppler GR. A Mindlin shell element that satisfies rigid-body requirements. *AIAA Journal* 1985; **23**:288–295.
32. Cantin G. Rigid body motions in curved finite elements. *AIAA Journal* 1970; **8**:1252–1255.
33. Scordelis AC, Lo KS. Computer analysis of cylindrical shells. *American Concrete Institute Journal* 1964; **61**:539–560.
34. MacNeal RH, Harder RL. A proposed standard set of problems to test finite element accuracy. *Finite Elements in Analysis and Design* 1985; **1**:3–20.
35. Kulikov GM. Analysis of initially stressed multilayered shells. *International Journal of Solids and Structures* 2001; **38**:4535–4555.

 